Hydration of Simple Carboxylic Acids from Infrared Spectra of HDO and Theoretical Calculations

Journal:	*The Journal of Physical Chemistry*
Manuscript ID:	jp-2011-00748u.R1
Manuscript Type:	Article
Date Submitted by the Author:	n/a
Complete List of Authors:	Śmiechowski, Maciej; Gdansk University of Technology, Department of Physical Chemistry Gojło, Emilia; Gdansk University of Technology, Department of Physical Chemistry Stangret, Janusz; Gdansk University of Technology, Department of Physical Chemistry

Hydration of Simple Carboxylic Acids from Infrared Spectra of HDO and Theoretical Calculations

Maciej Śmiechowski, Emilia Gojło, Janusz Stangret*

Department of Physical Chemistry, Chemical Faculty, Gdańsk University of Technology,

Narutowicza 11/12, 80-233 Gdańsk, Poland

E-mail address: msmiech@chem.pg.gda.pl

RECEIVED DATE:

* To whom correspondence should be addressed. Phone: (+48) 58 347 1283. Fax: (+48) 58 347 2694.

E-mail address: msmiech@chem.pg.gda.pl.

The hydration of carboxylic acids in dilute aqueous solutions is important for our understanding of their functioning in the biochemical context. Here we apply vibrational spectra of HDO isotopically diluted in H_2O to study this phenomenon, using the difference spectra method for analysis and interpretation of the results. The spectra of HDO affected by formic, acetic and propionic acid display characteristic component bands, significantly red-shifted from the bulk HDO band position. The appearance of these component bands is linked with isotopic substitution on the carboxylic acid molecule, which forms a short and strong hydrogen bond with a water molecule. Additionally, a charge separation due to the proton transfer in the neutral form of the complex leading to a contact ion pair formation may be inferred from the affected HDO spectra. Apart from the contraction of the principal acid-water hydrogen bond, it results in other major structural changes in the hydration shell, as revealed by Density Functional Theory (DFT) calculations of optimal geometries of aqueous clusters of the studied acids.

Keywords: Carboxylic acids, aqueous solutions, hydration, FTIR spectroscopy, DFT calculations.

Introduction

Carboxylic acids form an important class of biomolecules and their hydration in dilute aqueous solutions has important implications for our understanding of their role in the biochemical context. Owing to the presence of both an alkyl chain and a hydrophilic –COOH head group, carboxylic acids often experience a mixed type of hydration, i.e., the hydrophobic hydration of the alkyl chain combined with the hydrophilic hydration of the head group. The cooperative effects of both types of hydration are supposed to determine the overall interaction of the molecule with water.[1]

Carboxylic acids belong to moderately weak ones (pK_a = 3.75, 4.76, 4.87 for formic, acetic, and propionic acid, respectively)[2] and are mostly undissociated in an aqueous solution. Strong acids, upon dissolution in water, release the proton into the surrounding medium, giving rise to the hydrated proton species with unique properties. The debate, whether it is the so-called Eigen cation (H_3O^+) or the Zundel cation ($H_5O_2^+$) that correctly describes the hydrated individuum, now seems to reach a conclusion that H^+_{aq} forms a "fluxional defect" in the hydrogen-bonded (H-bonded) network of water[3] with proton transfer (PT) acts facilitated by complicated rearrangements of the H-bond network.[4] The existence of some intermediate forms, variously referred to as a "deformed Eigen" or "deformed Zundel" cation has been also proposed on the basis of computational and spectroscopic studies.[5-9]

Infrared spectra of aqueous solutions of strong acids are characterized by the so-called "continuum of absorption" (very broad, essentially structureless low-intensity absorption in the 3000-1000 cm^{-1} region). The concept of "extremely polarisable" hydrogen bonds was proposed by Zundel and his co-workers to justify its appearance.[10] However, in relatively dilute aqueous solutions of strong acids this region of the vibrational spectrum could be adequately resolved into analytical component bands.[7,8] For weaker acids (such as HCOOH) the intensity of the "continuum" is much weaker and the protons in the acid-water H-bonds are supposed to reside preferentially at the acid site, with the protonic polarisability being much lower.[11]

Although this picture of strong acid-water H-bonding with acid as proton donor and water as proton acceptor in the H-bond prevailed in the interpretation of infrared data,[11,12] the possibility of carboxylic

acids to form relatively stable ion pairs in water was also investigated.[13-20] Molecular dynamics (MD) simulations led to a conclusion that the formation of a contact ion pair (CIP) is the first step leading ultimately to the act of acid dissociation[16-18,20] (by contact ion pair we denote a structure, in which the acidic anion and the hydrated proton are directly adjacent after the occurrence of dissociation).

Simple carboxylic acids in aqueous environment have been thus far studied with diverse theoretical and experimental methods. Their aqueous clusters were investigated with static *ab initio* calculations,[14,15,19,21-26] as well as with matrix isolation vibrational spectroscopy[26] and mass spectrometry.[27] Aqueous solutions of carboxylic acids were studied computationally with MD[16-20,28,29] and Monte Carlo (MC) simulations.[30,31] Experimental studies of such solutions were mainly conducted with vibrational spectroscopy, both infrared[11,12] and Raman spectroscopy,[13,32-38] but also dielectric spectroscopy,[39] X-ray scattering studies[40] and volumetric measurements[41] were applied for this purpose.

Vibrational spectroscopy, although regarded as one of the best methods to study the solute hydration,[42] in the case of aqueous solutions of protic solutes faces the added complication of the presence of different –OH groups in the system, originating not exclusively from the water molecules. The spectroscopy of HDO isotopically diluted in H_2O (D_2O), which is widely considered an ideally suited method in hydration studies,[43] in this case offers no benefit by itself, since isotopic substitution in principle proceeds on all protic groups in the system. One of the possible solutions is the application of factor analysis techniques to the vibrational spectra of aqueous solutions, which allow extraction of spectra of chemically relevant species present in the system. This approach was already applied in the studies of aqueous carboxylic acids in H_2O.[12] Another approach, recently used in our group for the interpretation of HDO spectra, is to couple the band shape analysis with the static *ab initio* quantum mechanical (QM) calculations of optimal structures of small aqueous clusters. The ascription of component bands in the HDO spectra to particular hydrogen bonds in aqueous clusters is then possible resorting to empirical H-bond length vs. stretching frequency correlations.[44] Such approach proved successful in discriminating different deuterium substitutions in systems like aqueous solutions of the hydroxide anion[45] or anions of the phosphate(V) family.[46] Additionally, the aforementioned

"continuum" is absent in the HDO spectra in H_2O in the OD stretching range, due to isotopic decoupling of the OD oscillators from the surrounding bath.[9] Therefore, the application of HDO spectroscopy to study the hydration of carboxylic acids seems a preferable method.

For the present study, the three simplest homologous carboxylic acids, i.e., formic, acetic, and propionic acid have been selected. To study their hydration, we used vibrational (FTIR) spectroscopy of HDO isotopically diluted in aqueous solutions of the studied solutes in H_2O. The quantitative method of spectral data analysis formulated by Lindgren and coworkers, and independently in our laboratory,[47-49] allows separation of solute-affected water spectrum basing on the series of spectra measured at increasing concentration of the solute. The transformation of the obtained HDO band contour to water oxygen-oxygen distance probability distribution function, basing on the published procedure,[47,49] reveals also the structural state of the hydration spheres. To further link the structural and spectral data, we also applied static *ab initio* QM calculations of optimal structures of small aqueous clusters of the solutes in the gas phase and in the water solvent simulated by the polarizable continuum model (PCM).[50]

Experimental Section

Formic acid (80% aq., pure p.a.), acetic acid (pure p.a.) and propionic acid (97%) from POCh Poland were used as supplied. D_2O (99.84% isotopic purity) was provided by Institute of Nuclear Investigation, Poland. Stock solutions were prepared by dissolving weighted amounts of respective solutes in double-distilled water. The series of solutions were prepared by dissolving weighted amounts of respective stock solution in double-distilled water. The solution series of carboxylic acids included samples from the 0.1-1.0 mol·kg^{-1} molality range. The natural pH of the solutions was not adjusted and its range was 1.88-2.37 for formic acid, 2.40-2.89 for acetic acid and 2.46-2.94 for propionic acid. Sample solutions were made by adding 4% (by weight) of D_2O relative to H_2O and reference solutions by adding the same molar amounts of H_2O. Densities of the solutions were measured with an Anton Paar DMA 5000 density meter at 25.000±0.001 °C.

FTIR spectra were recorded on IFS 66 Bruker spectrometer. 256 scans were made with 4 cm^{-1} resolution. A cell with CaF_2 windows was employed. The path length was 0.0299 mm, as determined interferometrically. The spectrometer was purged with dry air free of carbon dioxide. The temperature, monitored by a thermocouple inside the cell, was kept at 25.0±0.1 °C by circulating thermostated water through mounting plates of the cell.

Spectral Data Analysis

The spectra have been handled and analyzed by commercial programs GRAMS/32 4.01 (Galactic Industries Corporation, Salem, USA) and RAZOR (Spectrum Square Associates, Inc., Ithaca, USA) run under GRAMS/32.

Spectral data have been analyzed following the published procedures, allowing the separation of the spectrum of solute-affected water, basing on the spectra of the entire solution series and the bulk HDO spectrum.[48,49] The algorithm is based on the assumption that water in solution may be divided into additive contributions of bulk (*b*) and solute-affected (*a*) water. The vibrational spectrum of the latter, ε_a, may be calculated for each wavenumber using Eq. (1a) from the pure HDO spectrum, ε_b, and the solution spectrum, ε, assuming that the "affected number", *N*, is known (its significance will be discussed below). In the infinite dilution limit ($m \rightarrow 0$) the bracketed fraction may be approximated by the derivative of molar absorptivity vs. molality as in Eq. (1b). In both equations *M* denotes the mean molar mass of water (H_2O + 4% D_2O).

$$\varepsilon_a = \frac{1}{NM}\left(\frac{\varepsilon - \varepsilon_b}{m}\right) + \varepsilon_b \qquad (1a)$$

$$\varepsilon_a = \frac{1}{NM}\left(\frac{\partial \varepsilon}{\partial m}\right)_{m=0} + \varepsilon_b \qquad (1b)$$

An approximation of the experimental spectra $\varepsilon(\nu_i)$ vs. molality *m* at each wavenumber ν_i by the least squares method allows the calculation of the respective derivative.

The *N* parameter is equal to the number of moles of water affected by one mole of solute in the infinite dilution conditions. The proper value of it is found basing on the published algorithm.[49] Briefly, the trial solute-affected water spectrum for a given *N* value is fitted using the baseline, analytical bands and the bulk water spectrum. The product of Gaussian and Lorentzian peak functions is normally used as the starting analytical band shape, but it might be replaced later by a pure function for a given band if the contribution of the other component is found negligible. The maximum value of *N*, for which the solute-affected water spectrum still contains a negligible amount of the bulk water spectrum is considered as the "true" value of *N* (usually, the threshold value for bulk water contribution is set at 0.5% of the total integrated intensity of the ε_a spectrum). The ε_a spectrum corresponding to this *N* is regarded as the "true" affected water spectrum. Thus, both unknowns are obtained simultaneously.

Computational Details

The model systems in the calculations were aqueous clusters $RCOOH(H_2O)_n$ (R = H, CH_3, C_2H_5, n = 1–8). Sixteen clusters were considered for each acid, and thus the total number of cluster structures discussed here is 48.

QM calculations were performed in the framework of Density Functional Theory (DFT), utilizing the hybrid B3LYP exchange-correlation functional with the 6-311++G(d,p) basis set.[51] All calculations were performed with the Gaussian 09 system.[52] *Tight* convergence criteria were used for optimizations. Vibrational analysis was performed on optimized clusters to check for absence of imaginary frequencies and thus confirm the existence of local energetic minima. Zero-point vibrational energies (ZPVE) and thermal corrections to energy, enthalpy and Gibbs free energy were simultaneously obtained during the vibrational analysis. The ZPVE values were empirically scaled by the recommended scale factor equal to 0.9877.[53]

Gas phase cluster structures were subsequently used as starting points for geometry optimization in the self-consistent reaction field approach. The polarizable continuum solvation model (PCM) in the integral equation formalism was used.[50] The atomic radii for molecular cavity definition were taken

from the UFF force field.[54] Additionally, the new SMD parameterization for PCM was used.[55] The united atom approach was not applied in the PCM calculations.

Results and Discussion

Figure 1a presents the molar absorptivity derivatives $(\partial\varepsilon/\partial m)_{m=0}$ obtained on the basis of the measured spectra for the solution series of the three studied acids (available as Supporting Information). These derivatives correspond to the linear regression of $\varepsilon(\nu)$ values vs. solution molality. Together with the bulk HDO spectrum, they were used to determine the solute-affected HDO spectra according to eq 1. Spectra of HDO affected by formic, acetic and propionic acids are shown in Figure 1b. The affected number was found to be almost constant for the three studied acids ($N = 3.9 \pm 0.1$). A similar value for the total number of acid-water interactions was obtained previously for dilute acetic acid-water mixtures in X-Ray diffraction experiments.[40] The decomposition of the affected spectra into analytical component bands is illustrated in Figure 2 and their most important parameters (excluding baseline correction bands) are gathered in Table 1.

As seen in Table 1, component band positions at maximum (ν°_{OD}) are similar for all the acids. Excluding the band at ~2125 cm^{-1} for acetic acid in Figure 2b (which arises from the uncompensated intramolecular absorption of the acid), other bands seem to correspond closely. In the case of acetic and propionic acids of very similar strength, the band positions are almost identical. For the stronger formic acid, a slight blue shift of the ~2550 cm^{-1} and the ~2430 cm^{-1} bands is apparent, accompanied by a red shift of the ~2260 cm^{-1} and the ~2050 cm^{-1} bands. Additionally, a well-developed band at ca. 1950 cm^{-1} is apparent for formic acid and is slightly less intense for acetic acid, while for propionic acid it is not observed.

As we have recently shown, analogous carboxylates display two component bands of affected HDO at ~2550 and ~2420 cm^{-1}.[55] These locations correspond well to those observed in this work. We previously interpreted them in terms of instantaneous charge localization on the carboxylate anion, with one oxygen

atom negatively charged as in the hydroxide anion (for which $\nu°_{OD}$ = 2437 cm^{-1})[45] and the other one resembling the carboxylic group in ketones (for which $\nu°_{OD}$ = 2540 cm^{-1}).[56] In an undissociated carboxylic acid molecule, the localization of the single and double bond is obvious and the band at ~2550 cm^{-1} may be ascribed to the water molecules H-bonded to the oxygen atom engaged in the C=O bond. This, however, does not justify the presence of the band at ~2430 cm^{-1}. The H-bond donated by the acid to the accepting water molecule may be suspected to be much stronger. For phosphoric(V) acid, an analogous H-bond gives rise to an HDO band at 2310 cm^{-1},[46] while for carboxylic acids in H_2O, a strong and short acid-water H-bond is responsible for the ν_{OH} band at ~3000 cm^{-1}.[12] The latter figure, transformed to OD intramolecular stretching frequency[57] gives $\nu°_{OD}$ = ~2280 cm^{-1}. Therefore, the ~2260 cm^{-1} band may be with high certainty ascribed to the C-O-D$^{\cdots}$OH$_2$ hydrogen bond. The appearance of the ~2430 cm^{-1} band in the carboxylic acid-affected HDO spectra will be discussed later.

The more elusive is the origin of the ~2625 cm^{-1} and ~2050 cm^{-1} bands. The former may be traced in the H_3PO_4-affected HDO spectrum, interpreted previously by us.[46] It has been ascribed to the water-acid H-bond to the acidic oxygen atom (i.e., the one that has the acidic proton directly bonded to it). The engagement in a strong H-bond via the acidic hydrogen makes this oxygen atom a poor electron pair donor and weakens the accepted H-bond in an anticooperative way. A similar H-bonding pattern for carboxylic acids is expected.

The remaining ~2050 cm^{-1} band (and also the ~1950 cm^{-1} one) is unusually red-shifted for a component band of the HDO spectrum. Previously, such situation was encountered by us only in the case of the H^+-affected HDO spectrum in strongly acidic solutions.[9] On the basis of the ab initio optimized cluster geometries, the possibility of the existence of the regular Eigen (H_3O^+) cation in such aqueous solutions was ruled out by the absence in the mentioned affected spectra of the characteristic OD stretching band ($\nu°_{OD}$ = ~2050 cm^{-1}), corresponding to strong H-bonds in the H_3O^+ first hydration sphere.[9] Its presence in the carboxylic acid-affected HDO spectra strongly suggests the possibility of existence of RCOO$^{-\cdots}$H$_3$O$^+$ CIPs in a measurable proportion. The resulting Eigen-type cation would then be responsible for the appearance of the ~2050 cm^{-1} band. Let us mention briefly that previous

experimental evidence supporting the existence of CIPs in aqueous solutions of carboxylic acids is rather scarce. They were indirectly detected in Raman spectra by splitting of the C–C stretching band only. These spectral features were observed solely in heavy water, so the higher acidity of carboxylic acids in D_2O was suggested as the possible explanation of the phenomenon.[13]

The tentative interpretation of the component bands in the carboxylic acid-affected HDO spectra outlined above may be strengthened in confrontation with electronic structure calculations. However, when such a comparison is made, a direct comparison of H-bond lengths' distribution is beneficial. The vibrational spectra of HDO in the OD stretching range may be transformed to the interatomic oxygen-oxygen distance probability distribution via generalization[49] of the well-known empirical distance-frequency relationships (see also below).[44] This provides a direct structure-spectrum relationship in terms of the H-bond length distribution in the affected solvent. The probability distributions resulting from the calculated affected spectra are shown in Figure 3 and compared to the bulk HDO case. It is evident that these curves are highly structured and once again discriminate between the very similar acetic and propionic acids and the stronger formic acid. The strongly red-shifted component bands in the affected spectra are responsible for the appearance of probability distribution features at ca. 2.53 Å and slightly above 2.6 Å, indicating the presence of short hydrogen bonds.

The existence of such strong and short hydrogen bonds may be verified in static QM calculations. Representative carboxylic acids aqueous clusters studied in this work are illustrated in Figure 4 (more are available as Supporting Information). While increasing the size of the clusters, we noticed that water molecules tend to form H-bonded rings with the acid molecule: one around the –OH group of the acid, one around the =O group and a third one connecting the two H-bonded networks in between the two functional groups. Adopting the previously proposed nomenclature, these rings are designated by counting the number of heavy (i.e., non-hydrogen) atoms.[58] Therefore, the cluster symbol XYZ denotes X heavy atoms forming the ring around the –OH site, Z heavy atoms forming the ring around the =O site, and Y heavy atoms forming the "bridging" ring. Each of the clusters presented was optimized for the three studied acids, however, no major structural changes were observed, apart from slight changes

in hydrogen bond lengths (see Table 2). The major difference in the gas phase between formic acid and the other two acids comes from the 474 cluster, which is a CIP for formic acid and neutral otherwise.

We found previously that the parameter most useful in the comparison with the experimental affected HDO spectra is the hydrogen bond length, measured by the interatomic oxygen-oxygen distance (R_{OO}). The R_{OO} value can be easily transformed to the OD band position of HDO (ν^{o}_{OD}) with the aid of empirical relations. Eq. (2) linking ν^{o}_{OD} to R_{OO} was established on the basis of vibrational spectra and neutron diffraction measurements on crystalline hydrates.[44]

$$\nu^{o}_{OD} / \mathrm{cm}^{-1} = 2727 - \exp[16.01 - 3.73(R_{OO} / \text{Å})] \quad (2)$$

Although this procedure seems like a roundabout route to the OD stretching frequency, which might as well be simply determined from QM frequency calculations, we found formerly that the stretching frequencies determined from the molecular geometry with the aid of the empirical relation (2) correlate much better with the experimental component bands.[9,45,46] The hydrogen bond lengths and the corresponding calculated frequencies (ν^{c}_{OD}) for the studied solutes are shown in Table 2, averaged over different molecular situations in all clusters (individual H-bond lengths are available in the Supporting Information). The hydrogen bond types encountered in the studied clusters in both neutral and contact ion pair form are schematically illustrated in Fig. 5.

The most noteworthy feature of our gas phase calculations is the existence of stable ion pairs (the 464, 474 and 574 structures for formic acid, and the 464 and 574 structures for the other acids). Previously investigated aqueous clusters of carboxylic acids were usually too small to allow for stable energetic minima corresponding to CIP structures.[21-25] However, explicit consideration of more solvating water molecules led to stable minima matching CIP and solvent–separated ion pair (SSIP) cases for both formic[14] and acetic acid[15] (by solvent–separated ion pair we denote a structure, in which at least one solvent molecule is positioned directly between the acidic anion and the hydrated proton). A formic acid cluster with 4 H_2O allowed for a stable SSIP structure, while an additional water molecule stabilized also the CIP structure.[14] For both types of ion pairs, the hydrated proton was clearly an Eigen-type cation (H_3O^+).[14,15]

The difference between the previous computational results and those obtained herein lies in the relative stability of the different isomers. To illustrate this, selected thermodynamic data for the studied clusters are included in Table 3. For example, the 464 cluster is a stable minimum on the potential energy surface (PES) at the B3LYP/6-311++G(d,p) level of theory and has a lower energy (including ZPVE) than the corresponding 464t cluster, which is also a stable local minimum at the same level. This is the first time that such an observation is made and all previously reported CIP or SSIP structures lay above the respective neutral clusters on the PES.[14,15] The 464t cluster is formed from 464 by a simple proton transfer through the inner ring of three water molecules. Such an arrangement for proton transfer was observed formerly in MD simulations.[16] At the same time, the reaction free energy for the 464t → 464 isomerisation in the gas phase is very close to zero (Table 3) and the process is almost at an ideal equilibrium. In a previous QM investigation, gas phase ΔG for isomerisation of acetic acid to an ion pair was also found to be –0.1 $kJ \cdot mol^{-1}$.[15] However, inclusion of the solvation free energy of the reactants obtained in the PCM/SMD approximation makes free energy more positive and the resulting equilibrium constant is on the order of 10^{-3} (Table 3).

The most interesting fact from the point of view of correlation with the spectral data is the dramatic structural change when going from neutral to CIP clusters. The C-$OH^{\cdots}OH_2$ hydrogen bond length is 2.615 Å in the gas phase for formic acid and 2.625 Å for the other acids (averaging over all the studied acid clusters, see Table 2, bond type IV). When in turn the cluster attains a CIP configuration, the resulting C-$O^{-\cdots}H_3O^+$ hydrogen bond shortens considerably to ~2.55 Å (see Table 2). The even more important difference between these two isomers is the equally pronounced shortening of the two hydrogen bonds formed with the other water molecules by the water molecule that is the proton acceptor from the acid (although the anion-cation H-bond still remains the shortest one of the three). Therefore, the Eigen-type H_3O^+ cation is a valid description of the formed individuum, as the H-bond length of 2.50-2.55 Å is characteristic for this case.[9]

Several concomitant phenomena due to the proton transfer in the CIP structures can be observed. The shortening of the two water-acid H-bonds to the C=O group, when it becomes a C–O^- group in a CIP

structure, is apparent (from ~2.87 Å for formic acid and ~2.85 Å for the other two acids to ~2.79-2.8 Å). It can be linked to the increased negative charge on the oxygen atom due to the charge separation in the CIP structure. The CHelpG charge[59] of the relevant oxygen atom changes from –0.590 in 464t to –0.748 in 464 (for formic acid). At the same time, the charge of the C-O-H oxygen atom changes from –0.689 in 464t to –0.795 after dissociation, with a similar change in the hydration structure. Apart from the obvious shortening of the H-bond connected with proton transfer, described above, the long H-bond donated by a water molecule to the –OH oxygen atom of the acid also shortens from 2.88-2.86 Å to ~2.73 Å, when the acid dissociates. Averaging over all three H-bonds to $C–O^-$ (two to the former C=O oxygen atom and one to the former –OH oxygen atom), the value ~2.77 Å is obtained for all three acids. Previously for analogous carboxylates we found a much more pronounced asymmetry in the hydrogen bond lengths between water and the two carboxylic oxygens, leading to instantaneous charge localization on the carboxylate anion visible also in the affected HDO spectra.[55] The charge differences reported previously for the two oxygens were on the order of 0.1,[55] which is observed here only for the neutral form of acidic clusters. Therefore, the presence of the hydronium cation leads to the marked charge delocalization in the CIP clusters, even though the cation itself is positioned asymmetrically with respect to the carboxylic anion in the 464, 474 and 574 clusters. However, the cation may transiently fluctuate within the water chain connecting the two carboxylic oxygens[16] and possible transition states with the hydronium cation located symmetrically between the two oxygens were reported before.[19] Consequently, this may lead to symmetrization of the interactions with the hydrating water and the picture observed in the static infrared spectra is a statistical average of the rapidly fluctuating Eigen cation.

The geometry of an aqueous cluster obtained in the gas phase is usually overstructured with respect to the situation in the solvent. We found previously that the application of the PCM approach to solvation provides much better agreement with the interatomic oxygen-oxygen distances obtained from the experimental spectra.[9,45,46] Also here, the H-bond lengths obtained with PCM are greater than the respective gas phase values, with the SMD model systematically predicting longer H-bonds on average

than the UFF atomic radii-based model (Table 2). The main deficiency of the UFF model is the lack of Eigen-type CIPs for acetic and propionic acids (clusters 464, 474, and 574). The SMD model performs better in this respect, failing to predict a CIP structure only for 474 (the same as in the gas phase results described above).

The average H-bond lengths, especially those obtained using the PCM/SMD approach, can now enable us to thoroughly interpret the observed analytical bands in the carboxylic acid-affected HDO spectra. Especially the structural changes between neutral and CIP clusters are reflected as equally pronounced changes in the position of the analytical component bands. The band positions at maximum after empirical transformation to the intermolecular oxygen-oxygen distance (Table 1) can be directly compared with the respective average distances obtained from QM calculations (Table 2).

As already mentioned above, the proton transfer from acid to water results in a red shift of the band position from ~2260 cm^{-1} to ~2050 cm^{-1} and the decrease of the H-bond length from 2.62-2.65 Å to ~2.54 Å, which is adequately reproduced in the PCM/SMD calculations, even with respect to the difference between formic acid and the other two acids. Simultaneously the bands at ~2625 cm^{-1} and ~2550 cm^{-1} shift to ~2430-2440 cm^{-1}, in the latter case from the position typical to the C=O group to the position typical to a negatively charged $C\text{-}O^-$ group.[55] This time the agreement with QM calculations is less impressive, however, the characteristic changes in H-bond lengths in this process are preserved, with H-bonds from the calculations generally shorter on average than the values obtained from the experimental band positions, especially for the two blue-shifted bands.

As all these bands are observed simultaneously in a static vibrational spectrum, equilibrium between the neutral and the CIP structure must be present. At the very least, the lifetime of each species should be longer than the characteristic time of the OD stretching vibration (~13.3 fs). Actually, the lifetime of the CIP form as predicted from MD simulations is much longer. The estimation based on Car-Parrinello MD was ca. 0.2-0.3 ps,[16] although it was also termed a "metastable intermediate" only.[17] The deprotonation of formic acid (FA) could also be followed by subsequent reprotonation in ~0.7 ps, leading through a SSIP intermediate and with proton transfer facilitated by a ring of 3 water molecules[16]

(cf. the arrangement of water molecules in the clusters 464 and 464t). In a single classical MD simulation with an algorithm allowing proton transfer acts, frequent proton shuttling between acetic acid and H-bonded water molecule was observed and this process seemed to be driven by environmental fluctuations.[20] Therefore, the observation of the OD stretching bands characteristic for CIP structures is entirely possible.

The actual proportion of the CIP to neutral form of the acid may be obtained from integrated intensities of the respective component bands, viz. ~2260 cm^{-1} and ~2050 cm^{-1}. However, the presence of an additional band at ~1950 cm^{-1} for formic and acetic acid makes such comparison difficult. This band most probably reflects the asymmetry of the Eigen cation formed in a CIP structure and its integrated intensity grows with increasing acid strength. On the other hand, the absolute value of this intensity is uncertain, as the band is located at the edge of the studied region and is artificially broadened in the fitting procedure to account for baseline corrections. Therefore, only for propionic acid a truly meaningful integrated intensity comparison may be performed. Before such a comparison is made, the intensities have to be rescaled taking into account the well-known effect that the integrated intensity of the HDO stretching bands increases approximately linearly with a shift to lower wavenumbers.[60,61] The general form of these relationships is expressed in Eq. (3), where the zero-intensity reference point ν°_{OD} = 2727 cm^{-1} is the gas phase OD stretching band position.[62]

$$I = C\cdot(2727 - \nu^{\circ}_{OD}) \quad (3)$$

On this basis, both bands' intensities were rescaled to their hypothetical values at the bulk HDO band center of gravity (2505 cm^{-1}) using Eq. (4) before calculating their ratio.

$$I^{c} = I\,\frac{2727 - 2505}{2727 - \nu^{\circ}_{OD}} \quad (4)$$

After such procedure the proportion of CIPs in aqueous solution as measured by the corrected intensity ratio of the two characteristic bands (I^{c}_{2050} / I^{c}_{2260} + I^{c}_{2050}) is ~12% for propionic acid. The proportion of CIPs basing on the PCM/SMD value of ΔG°_{aq} (Table 3) is an order of magnitude lower and amounts ~0.9%. Results comparable to our experimental data were obtained in CPMD simulations,

where the free-energy barrier for dissociation of neutral formic acid to CIP was ~4 kcal·mol^{-1}.[16] In a different study, the proportion of the CIP forms was estimated at ~3%.[20] In the latter case, the pH of the simulated solution was equal to 1, so a shift of the dissociation equilibrium towards the neutral form might be expected in comparison to our results. All these figures are much higher than the dissociation degree of propionic acid, which is ca. 0.37% at the standard concentration of 1 mol·dm^{-3}. However, this might be expected if the CIP formation is the first step in the proton transfer away from the anion that ultimately results in the acid dissociation.[16-18,20]

Conclusions

The hydration of the –COOH group viewed from the perspective of the affected HDO spectra might be roughly described as an "additive" phenomenon. In particular, the hydration of the neutral form of the acid is well described as a combination of HDO affected by the C=O group and the C-OH group. The former was previously studied by us in aqueous solutions of simple ketones (acetone and 2-butanone)[56] and gives rise to a component band at $\nu°_{OD} \approx 2540$ cm^{-1}, as also observed here. In turn, two component bands are attributable to the C-OH group affected HDO. The C-OH hydrogen bond to water gives rise to a component at ca. ~2260 cm^{-1} (cf. analogous P-OH hydrogen bond to water in aqueous phosphoric(V) acid at 2310 cm^{-1})[46], while the H-bond from water to the C-OH oxygen atom is accountable for a component at 2625 cm^{-1} (also here there is a close correspondence to our previous study of H_3PO_4).[46] Water engaged in hydrophobic hydration of the alkyl chain is expected to contribute to the band at ~2540 cm^{-1}, as evidenced before for aqueous *sec*-butylamine.[1] The increase of the integrated intensity of this band for acetic and propionic acids with respect to formic acid (Table 2) seems to confirm this hypothesis.

For the contact ion pair isomer of a carboxylic acid, the component bands characteristic to the C-O$^-$ group and the Eigen form of the hydrated proton (H_3O^+) are visible in the spectra. The latter was previously not found by us in the strongly acidic solutions, where the "deformed Zundel" form of the hydrated proton prevails.[9] However, the characteristic $\nu°_{OD}$ value, predicted for it on the basis of ab

initio calculations[9] (~2050 cm^{-1}) is readily identified in the present affected HDO spectra (Table 1). In turn, the hydration of the C-O^- group is closely related to the hydration of hydroxide anion (OH^-). The negative charge on the oxygen atom causes a red shift of the OD stretching vibration and the value found previously for OH^- (2437 cm^{-1})[45] and carboxylate anions[55] is strikingly close to the component band position at 2430-2440 cm^{-1} found in this work.

The presence of both sets of the discussed component bands in the affected HDO spectra implies that the interaction of the carboxylic acid with the hydrating water molecules leads to the formation of contact ion pairs in an appreciable proportion (~12% as inferred from the respective bands' integrated intensities), in agreement with numerous MD studies.[16-18,20] The neutral to CIP interconversion in aqueous clusters seems to be facilitated by a ring of three water molecules, as also evidenced by the recent MD study.[16] This process ultimately leads to the acid dissociation and its equilibrium constant obtained in the PCM/SMD approximation is on the order of 10^{-3} (Table 3), at least an order of magnitude greater than the macroscopic acid dissociation constant.[2] Apart from the computational evidence, the changes in the hydration structure between the neutral and CIP acid forms are directly visible in the affected HDO spectra, as mentioned above, which offer possibly the first experimental proof that such equilibrium actually exists in aqueous solution, since only some indirect clues were reported before.[13]

Acknowledgments. This work was supported from the Republic of Poland scientific funds as a research project, within grant no. N N204 3799 33. Calculations were carried out at the Academic Computer Center in Gdańsk (TASK).

Supporting Information Available: Experimental spectra of the studied aqueous solutions in the OD stretching range of HDO. Gas phase optimized structures of the carboxylic acids' aqueous clusters not included in Figure 4. Individual hydrogen bond lengths in the optimized aqueous clusters. This material is available free of charge via the Internet at http://pubs.acs.org.

References

(1) Gojło, E.; Śmiechowski, M.; Stangret, J. *J. Mol. Struct.* **2005**, *744-747*, 809.

(2) Lide, D. R., Ed. *CRC Handbook of Chemistry and Physics*, 90th Ed., CRC Press, Boca Raton, FL, 2010, p. 8–42.

(3) Marx, D.; Tuckerman, M. E.; Hutter, J.; Parrinello, M. *Nature* **1999**, *397*, 601.

(4) Voth, G. A. *Acc. Chem. Res.* **2006**, *39*, 143.

(5) Botti, A.; Bruni, F.; Ricci, M. A.; Soper, A. K. *J. Chem. Phys.* **2006**, *124*, 014508.

(6) Asthagiri, D.; Pratt, L. R.; Kress, J. D. *Proc. Natl. Acad. Sci. U.S.A.* **2005**, *102*, 6704.

(7) Stoyanov, E. S.; Stoyanova, I. V.; Reed, C. A. *J. Am. Chem. Soc.* **2010**, *132*, 1484.

(8) Śmiechowski, M.; Stangret, J. *J. Mol. Struct.* **2008**, *878*, 104.

(9) Śmiechowski, M.; Stangret, J. *J. Chem. Phys.* **2006**, *125*, 204508.

(10) Zundel, G. In *The Hydrogen Bond - Recent Developments in Theory and Experiments*; Schuster, P.; Zundel, G.; Sandorfy, C., Eds.; North-Holland: Amsterdam, 1976; Vol. 2, pp 683-766.

(11) Leuchs, M.; Zundel, G. *J. Chem. Soc. Faraday Trans. II* **1980**, *76*, 14.

(12) Max, J.-J.; Chapados, C. *J. Phys. Chem. A* **2004**, *108*, 3324.

(13) Génin, F.; Quilès, F.; Burneau, A. *Phys. Chem. Chem. Phys.* **2001**, *3*, 932.

(14) Chuchev, K.; BelBruno, J. J. *J. Mol. Struct. (Theochem)* **2006**, *763*, 199.

(15) Yamabe, S.; Tsuchida, N. *J. Comput. Chem.* **2003**, *24*, 939.

(16) Lee, J.-G.; Asciutto, E.; Babin, V.; Sagui, C.; Darden, T.; Roland, C. *J. Phys. Chem. B* **2006**, *110*, 2325.

(17) Park, J. M.; Laio, A.; Iannuzzi, M.; Parrinello, M. *J. Am. Chem. Soc.* **2006**, *128*, 11318.

(18) Thomas, V.; Maurer, P.; Iftimie, R. *J. Phys. Chem. B* **2010**, *114*, 8147.

(19) Wei, D.; Truchon, J.-F.; Sirois, S.; Salahub, D. *J. Chem. Phys.* **2002**, *116*, 6028.

(20) Gu, W.; Frigato, T.; Straatsma, T. P.; Helms, V. *Angew. Chem. Int. Ed.* **2007**, *46*, 2939.

(21) Aloisio, S.; Hintze, P. E.; Vaida, V. *J. Phys. Chem. A* **2002**, *106*, 363.

(22) Zhou, Z.; Shi, Y.; Zhou, X. *J. Phys. Chem. A* **2004**, *108*, 813.

(23) Priem, D.; Ha, T.-K.; Bauder, A. *J. Chem. Phys.* **2000**, *113*, 169.

(24) Hsieh, Y.-H.; Weinberg, N.; Yang, K.; Kim, C.-K.; Shi, Z.; Wolfe, S. *Can. J. Chem.* **2005**, *83*, 769.

(25) Gao, Q.; Leung, K. T. *J. Chem. Phys.* **2005**, *123*, 074325.

(26) George, L.; Sander, W. *Spectrochim. Acta A* **2004**, *60*, 3225.

(27) Yamamoto, K.; Nishi, N. *J. Am. Chem. Soc.* **1990**, *112*, 549.

(28) Ruderman, G.; Caffarena, E. R.; Mogilner, I. G.; Tolosa, E. J. *J. Solution Chem.* **1998**, *27*, 935.

(29) Billeter, S. R.; van Gunsteren, W. F. *J. Phys. Chem. A* **2000**, *104*, 3276.

(30) SanRomán–Zimbrón, M. L.; Ortega–Blake, I. *J. Chem. Phys.* **1997**, *107*, 3253.

(31) Iftimie, R.; Salahub, D.; Wei, D.; Schofield, J. *J. Chem. Phys.* **2000**, *113*, 4852.

(32) Nishi, N.; Nakabayashi, T.; Kosugi, K. *J. Phys. Chem. A* **1999**, *103*, 10851.

(33) Kosugi, K.; Nakabayashi, T.; Nishi, N. *Chem. Phys. Lett.* **1998**, *291*, 253.

(34) Ng, J. B.; Shurvell, H. F. *J. Phys. Chem.* **1987**, *91*, 496.

(35) Tanaka, N.; Kitano, H.; Ise, N. *J. Phys. Chem.* **1990**, *94*, 6290.

(36) Tanaka, N.; Kitano, H.; Ise, N. *J. Phys. Chem.* **1991**, *95*, 1503.

(37) Semmler, J.; Irish, D. E. *J. Solution Chem.* **1988**, *17*, 805.

(38) Waldstein, P.; Blatz, L. A. *J. Phys. Chem.* **1967**, *71*, 2271.

(39) Kaatze, U.; Menzel, K.; Pottel, R. *J. Phys. Chem.* **1991**, *95*, 324.

(40) Takamuku, T.; Kyoshoin, Y.; Noguchi, H.; Kusano, S.; Yamaguchi, T. *J. Phys. Chem. B* **2007**, *111*, 9270.

(41) Granados, K.; Gracia-Fadrique, J.; Amigo, A.; Bravo, R. *J. Chem. Eng. Data* **2006**, *51*, 1356.

(42) Verrall, R.E.; Lilley, T.H.; Conway, B.E.; Luck, W.A.P. In *Water, a Comprehensive Treatise*, Franks, F., Ed., Plenum, New York, 1973, Vol. 3.

(43) Falk, M.; Ford, T. A. *Can. J. Chem.* **1966**, *44*, 1699.

(44) Berglund, B.; Lindgren, J.; Tegenfeldt, J. *J. Mol. Struct.* **1978**, *43*, 179.

(45) Śmiechowski, M.; Stangret, J. *J. Phys. Chem. A* **2007**, *111*, 2889.

(46) Śmiechowski, M.; Gojło, E.; Stangret, J. *J. Phys. Chem. B* **2009**, *113*, 7650.

(47) Kristiansson, O.; Lindgren, J.; de Villepin, J. *J. Phys. Chem*. **1988**, *92*, 2680.

(48) Stangret, J. *Spectrosc. Lett*. **1988**, *21*, 369.

(49) Stangret, J.; Gampe, T. *J. Phys. Chem. B* **1999**, *103*, 3778.

(50) Tomasi, J.; Mennucci, B.; Cancès, M. T. *J. Mol. Struct. (Theochem)* **1999**, *464*, 211.

(51) Stephens, P. J.; Devlin, F. J.; Chabalowski, C. F.; Frisch, M. J. *J. Phys. Chem.* **1994**, *98*, 11623.

(52) Gaussian 09, Revision A.02, Frisch, M. J.; Trucks, G. W.; Schlegel, H. B.; Scuseria, G. E.; Robb, M. A.; Cheeseman, J. R.; Scalmani, G.; Barone, V.; Mennucci, B.; Petersson, G. A.; Nakatsuji, H.; Caricato, M.; Li, X.; Hratchian, H. P.; Izmaylov, A. F.; Bloino, J.; Zheng, G.; Sonnenberg, J. L.; Hada, M.; Ehara, M.; Toyota, K.; Fukuda, R.; Hasegawa, J.; Ishida, M.; Nakajima, T.; Honda, Y.; Kitao, O.; Nakai, H.; Vreven, T.; Montgomery, Jr., J. A.; Peralta, J. E.; Ogliaro, F.; Bearpark, M.; Heyd, J. J.; Brothers, E.; Kudin, K. N.; Staroverov, V. N.; Kobayashi, R.; Normand, J.; Raghavachari, K.; Rendell, A.; Burant, J. C.; Iyengar, S. S.; Tomasi, J.; Cossi, M.; Rega, N.; Millam, N. J.; Klene, M.; Knox, J. E.; Cross, J. B.; Bakken, V.; Adamo, C.; Jaramillo, J.; Gomperts, R.; Stratmann, R. E.; Yazyev, O.; Austin, A. J.; Cammi, R.; Pomelli, C.; Ochterski, J. W.; Martin, R. L.; Morokuma, K.; Zakrzewski, V. G.; Voth, G. A.; Salvador, P.; Dannenberg, J. J.; Dapprich, S.; Daniels, A. D.; Farkas, Ö.; Foresman, J. B.; Ortiz, J. V.; Cioslowski, J.; Fox, D. J. Gaussian, Inc., Wallingford CT, 2009.

(53) Merrick, J. P.; Moran, D.; Radom, L. *J. Phys. Chem. A* **2007**, *111*, 11683.

(54) Rappe, A. K.; Casewit, C. J.; Colwell, K. S.; Goddard III, W. A.; Skiff, W. M. *J.Am. Chem. Soc.* **1992**, *114*, 10024.

(55) Gojło, E.; Śmiechowski, M.; Panuszko, A.; Stangret, J. *J. Phys. Chem. B* **2009**, *113*, 8128.

(56) Gojło, E.; Gampe, T.; Krakowiak, J.; Stangret, J. *J. Phys. Chem. A* **2007**, *111*, 1827.

(57) Berglund, B.; Lindgren, J.; Tegenfeldt, J. *J. Mol. Struct.* **1978**, *43*, 169.

(58) Pu, L.; Wang, Q.; Zhang, Y.; Miao, Q.; Kim, Y. S.; Zhang, Z. B. *Adv. Quantum Chem.* **2008**, *54*, 271.

(59) Breneman, C. M.; Wiberg, K. B. *J. Comp. Chem.* **1990**, *11*, 361.

(60) Glew, D. N.; Rath, N. S. *Can. J. Chem.* **1971**, *49*, 837.

(61) Bergström, P.-Å.; Lindgren, J.; Kristiansson, O. *J. Phys. Chem.* **1991**, *95*, 8575.

(62) Morozow, W. P.; Kwasha, N. T.; Caune, A. J.; Lisowienko, W. A. *Opt. Spectrosc.* **1963**, *15*, 617.

TABLE 1: Selected Parameters of Analytical Component Bands from Decomposition of Spectra of HDO Affected by the Studied Carboxylic Acids

Solute	ν^{o}_{OD} [a]	fwhh [b]	I [c]	R_{OO} [d]
HCOOH	2627	76	916	3.058
	2558	104	2798	2.917
	2444	200	3680	2.779
	2212	227	1570	2.618
	2037	88	287	2.540
	1956	182	874	2.510
CH_3COOH	2625	86	1066	3.052
	2546	122	4818	2.899
	2432	143	2683	2.768
	2261	191	1587	2.645
	2052	101	356	2.546
	1923	176	494	2.499
C_2H_5COOH	2625	83	636	3.052
	2550	125	4844	2.905
	2432	166	2568	2.768
	2264	206	1399	2.647
	2054	111	278	2.546

[a] Band position at maximum (cm^{-1}). [b] Full-width at half-height (cm^{-1}). [c] Integrated intensity ($dm^{-3} \cdot mol^{-1} \cdot cm^{-2}$). [d] Interatomic oxygen-oxygen distance obtained from ν^{o}_{OD} by an empirical relation.[44]

TABLE 2: Average Hydrogen Bond Lengths in Different Structural Situations for the Optimized Aqueous Clusters of Carboxylic Acids (R-COOH)

solute	assignment[a]	gas		SMD		UFF	
		m[b]	R_{OO}[c]	m[b]	R_{OO}[c]	m[b]	R_{OO}[c]
R = H	I) C-O(H)···H-OH	7	2.885(69)	5	2.911(29)	5	2.884(25)
	II) C=O···H-OH	12	2.866(94)	11	2.883(63)	11	2.868(62)
	III) C-O$^-$···H-OH	9	2.771(34)	9	2.806(46)	9	2.788(33)
	IV) C-OH···OH_2	13	2.615(55)	13	2.620(25)	13	2.622(35)
	V) OH_3^+···O	9	2.545(57)	9	2.567(25)	9	2.547(48)
R = CH_3	I) C-O(H)···H-OH	8	2.859(54)	7	2.919(85)	9	2.906(90)
	II) C=O···H-OH	14	2.847(85)	13	2.864(52)	18	2.857(50)
	III) C-O$^-$···H-OH	6	2.775(40)	6	2.796(36)	0	
	IV) C-OH···OH_2	14	2.626(70)	14	2.641(28)	16	2.631(48)
	V) OH_3^+···O	6	2.546(77)	6	2.565(60)	0	
R = C_2H_5	I) C-O(H)···H-OH	8	2.857(56)	7	2.921(88)	9	2.904(93)
	II) C=O···H-OH	14	2.845(83)	13	2.859(46)	18	2.856(49)
	III) C-O$^-$···H-OH	6	2.775(34)	6	2.799(35)	0	
	IV) C-OH···OH_2	14	2.625(68)	14	2.647(29)	16	2.634(48)
	V) OH_3^+···O	6	2.548(86)	6	2.565(71)	0	

[a] The hydrogen bond in question is marked by ellipsis, the Roman numbers refer to Fig. 5. [b] Total number of hydrogen bonds of specific type in all clusters of a given solute. [c] Average intermolecular oxygen-oxygen distance (Å); standard deviation (as final digits of the value) given in parentheses.

TABLE 3: Selected Thermodynamic Data for the Optimized Aqueous Clusters of Carboxylic Acids (R-COOH)

solute	cluster[a]	E_0[b]	ΔE_0[c]	ΔH_{298}[d]	ΔG_{298}[e]	K[f]	ΔG_{aq}[g]	K_{aq}[h]
R = H	464	-648.488809	-7.7	-11.5	0.1	0.95	13.0	$5.2 \cdot 10^{-3}$
	464t	-648.485881						
R = CH_3	464	-687.796377	-3.2	-6.2	1.4	0.57	13.9	$3.6 \cdot 10^{-3}$
	464t	-687.795170						
R = C_2H_5	464	-727.092638	-6.7	-9.6	-0.4	1.18	11.8	$8.6 \cdot 10^{-3}$
	464t	-727.090103						

[a] The clusters are identified by their symbols from Figure 4. [b] Total energy, including scaled zero-point vibrational energy (hartree). [c] Energy difference between 464 and 464t at 0 K ($kJ \cdot mol^{-1}$). [d] Enthalpy difference between 464 and 464t at 298 K ($kJ \cdot mol^{-1}$). [e] Gibbs free energy difference between 464 and 464t at 298 K ($kJ \cdot mol^{-1}$). [f] Equilibrium constant for the 464t → 464 process at 298 K. [g] Gibbs free energy difference between 464 and 464t in aqueous solution (SMD solvation model) at 298 K ($kJ \cdot mol^{-1}$). [h] Equilibrium constant for the 464t → 464 process in aqueous solution (SMD solvation model) at 298 K.

Figure 1. (a) The derivatives $(\partial\varepsilon/\partial m)_{m=0}$ and (b) the affected HDO spectra based on them for formic (green line), acetic (red line) and propionic (blue line) acid. The bulk HDO spectrum indicated with black dashed line in (b).

Figure 2. The spectra of HDO affected by (a) formic (green line), (b) acetic (red line) and (c) propionic (blue line) acid, and their decomposition into analytical bands (dashed lines).

Figure 3. Interatomic oxygen-oxygen distance distribution obtained from the affected HDO spectra in Fig. 1(b) for formic (green line), acetic (red line) and propionic (blue line) acid. The bulk HDO distance distribution indicated with dashed line.

Figure 4. Representative R-COOH clusters (R = H, CH_3, C_2H_5) studied in this work with both neutral and contact ion pair arrangement, optimized in the gas phase at the B3LYP/6-311++G(d,p) level for R = H. Hydrogen bonds indicated by thin lines, light grey spheres indicate hydrogens, dark grey – carbons, red – oxygens, blue – R substituents. See text for the explanation of cluster symbols.

Figure 5. Schematic R-COOH aqueous clusters in (a) neutral and (b) contact ion pair arrangement, with hydrogen bonds indicated by dashed lines. The Roman numbers over hydrogen bonds refer to hydrogen bond types listed in Table 2.

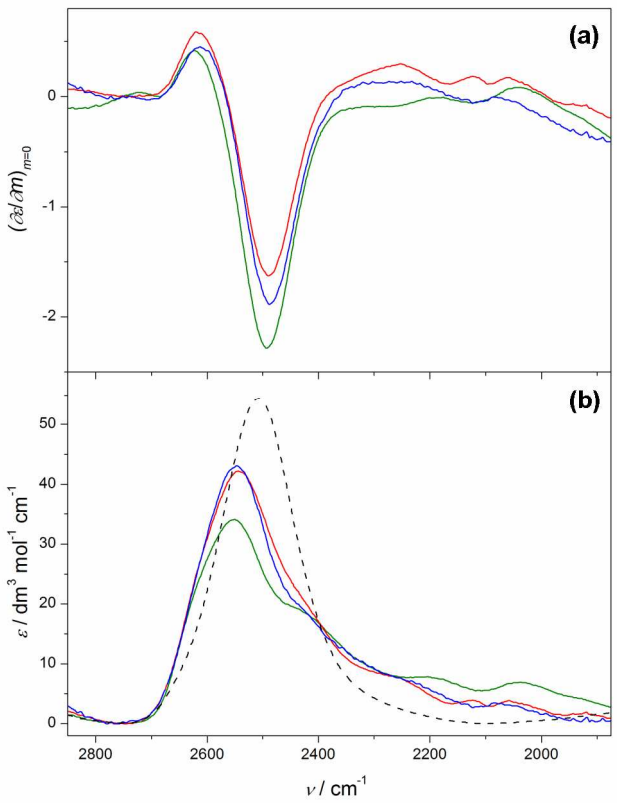

Figure 1. (a) The derivatives $(\partial\varepsilon/\partial m)_{m=0}$ and (b) the affected HDO spectra based on them for formic (green line), acetic (red line) and propionic (blue line) acid. The bulk HDO spectrum indicated with black dashed line in (b).

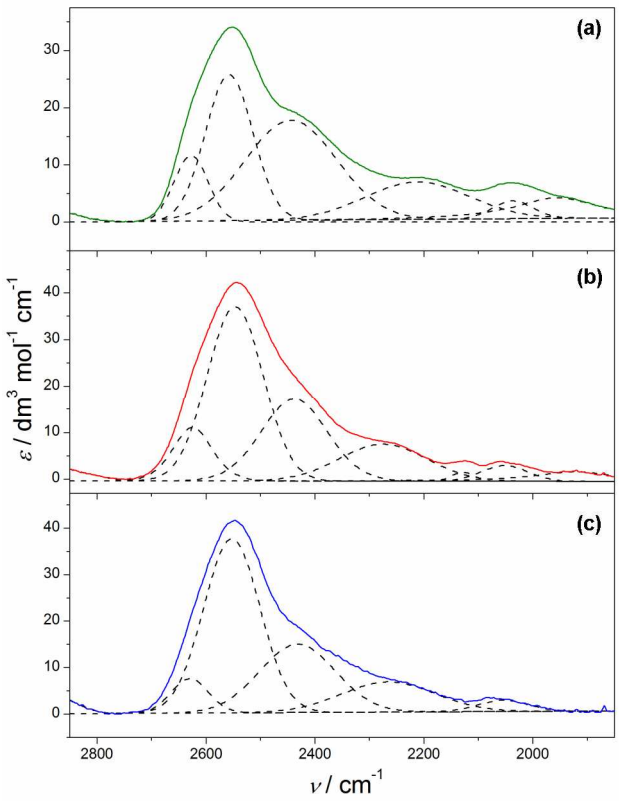

Figure 2. The spectra of HDO affected by (a) formic (green line), (b) acetic (red line) and (c) propionic (blue line) acid, and their decomposition into analytical bands (dashed lines).

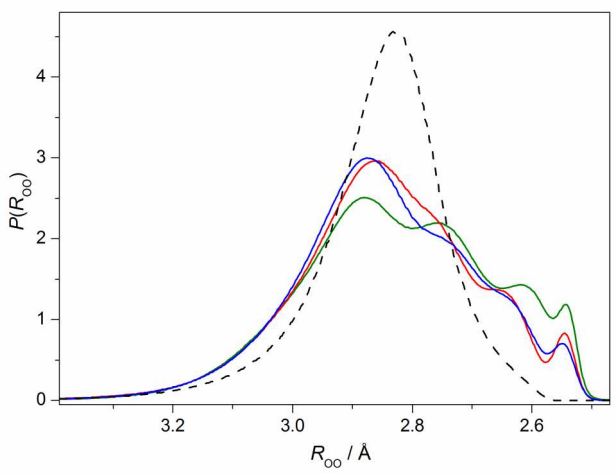

Figure 3. Interatomic oxygen-oxygen distance distribution obtained from the affected HDO spectra in Fig. 1(b) for formic (green line), acetic (red line) and propionic (blue line) acid. The bulk HDO distance distribution indicated with dashed line.

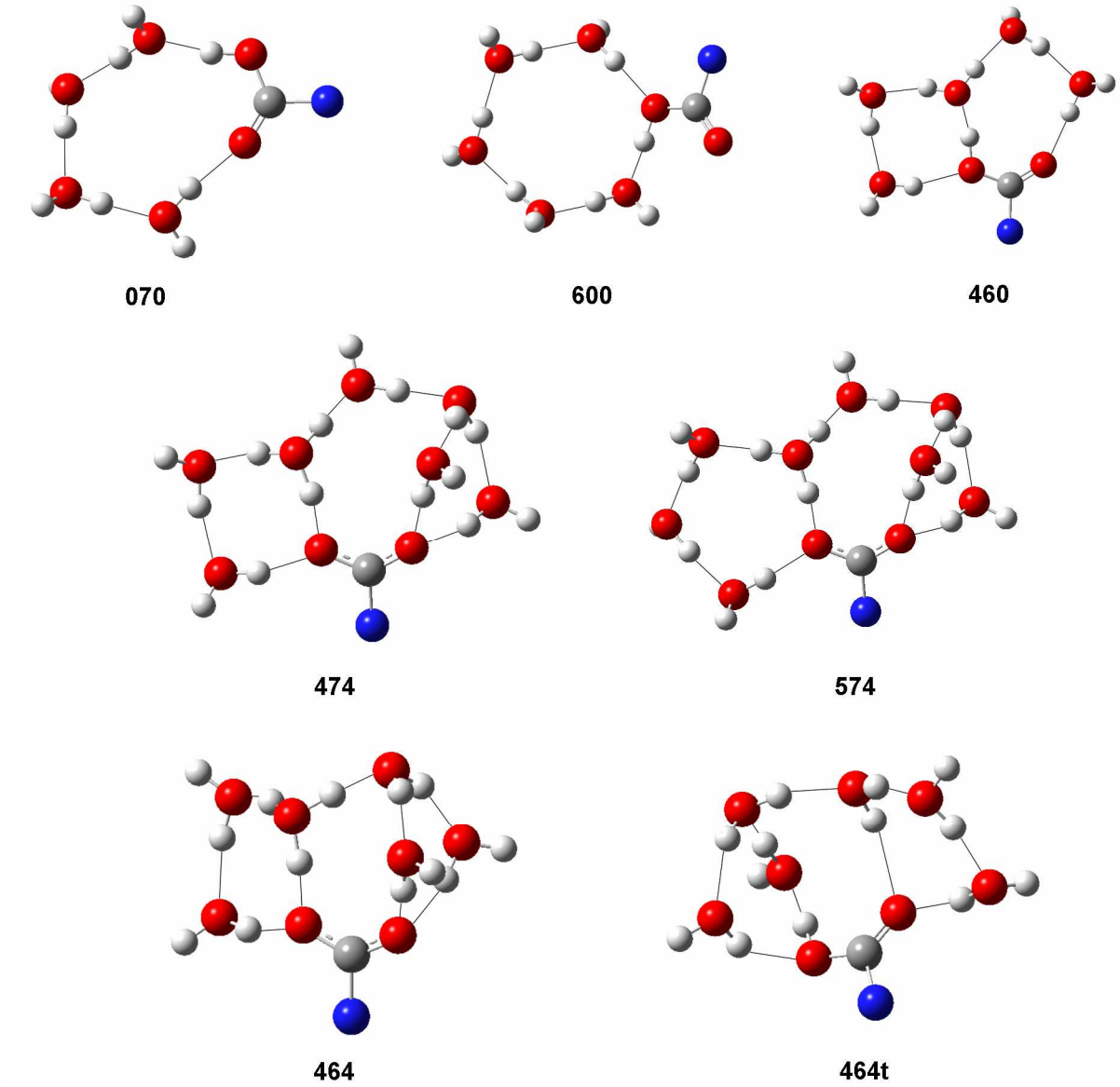

Figure 4. Representative R-COOH clusters (R = H, CH_3, C_2H_5) studied in this work with both neutral and contact ion pair arrangement, optimized in the gas phase at the B3LYP/6-311++G(d,p) level for R = H. Hydrogen bonds indicated by thin lines, light grey spheres indicate hydrogens, dark grey – carbons, red – oxygens, blue – R substituents. See text for the explanation of cluster symbols.

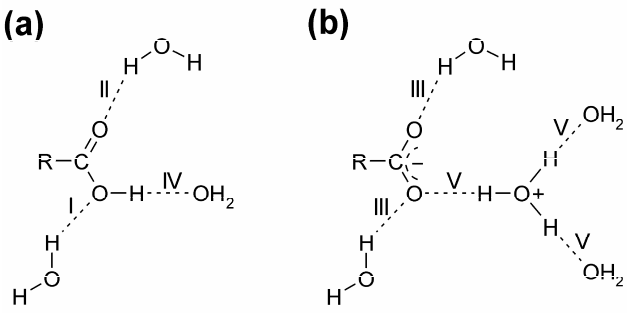

Figure 5. Schematic R-COOH aqueous clusters in (a) neutral and (b) contact ion pair arrangement, with hydrogen bonds indicated by dashed lines. The Roman numbers over hydrogen bonds refer to hydrogen bond types listed in Table 2.

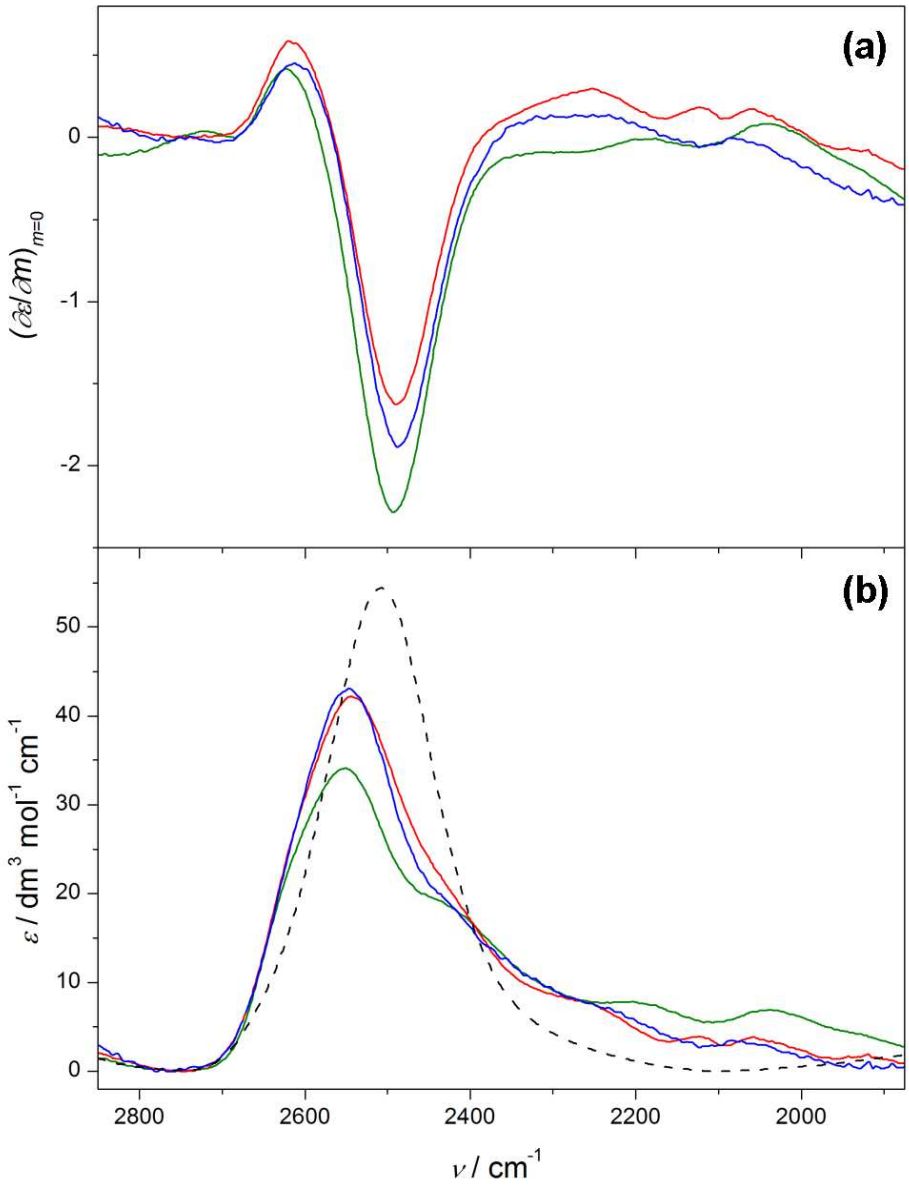

Figure 1. (a) The derivatives (∂ε/∂m)m=0 and (b) the affected HDO spectra based on them for formic (green line), acetic (red line) and propionic (blue line) acid. The bulk HDO spectrum indicated with black dashed line in (b).

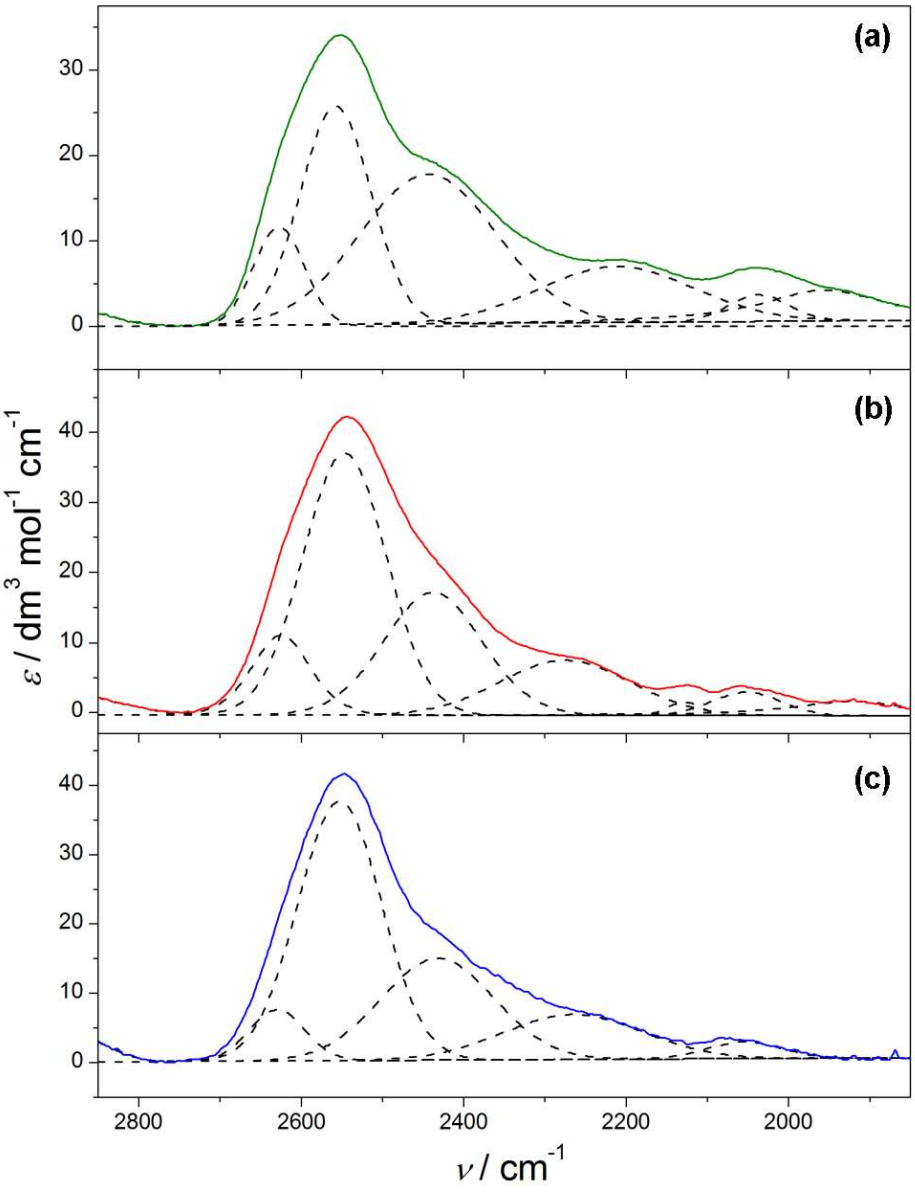

Figure 2. The spectra of HDO affected by (a) formic (green line), (b) acetic (red line) and (c) propionic (blue line) acid, and their decomposition into analytical bands (dashed lines).

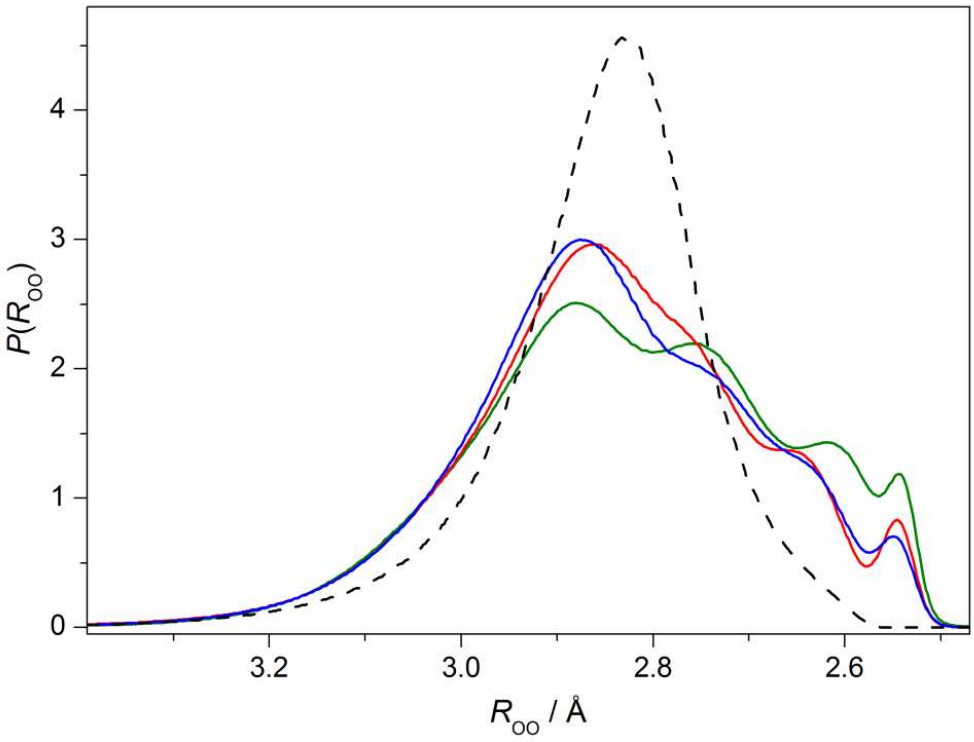

Figure 3. Interatomic oxygen-oxygen distance distribution obtained from the affected HDO spectra in Fig. 1(b) for formic (green line), acetic (red line) and propionic (blue line) acid. The bulk HDO distance distribution indicated with dashed line.

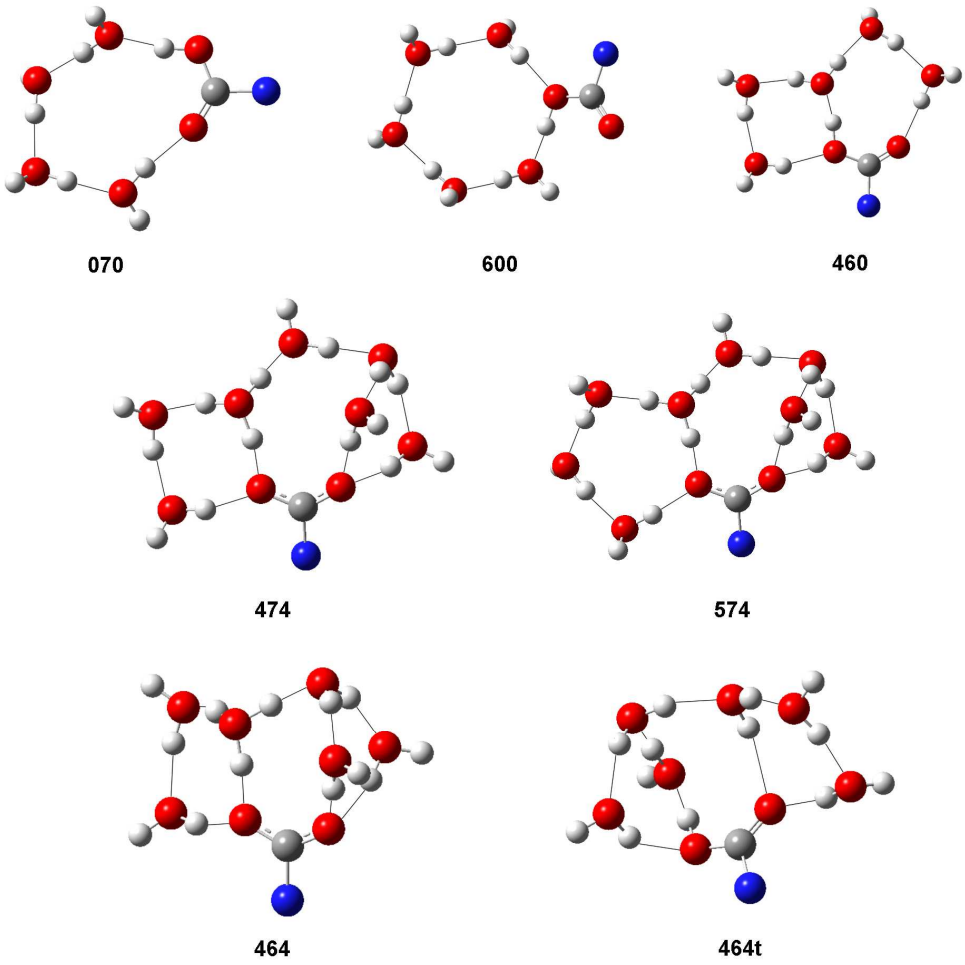

Figure 4. Representative R-COOH clusters (R = H, CH_3, C_2H_5) studied in this work with both neutral and contact ion pair arrangement, optimized in the gas phase at the B3LYP/6-311++G(d,p) level for R = H. Hydrogen bonds indicated by thin lines, light grey spheres indicate hydrogens, dark grey – carbons, red – oxygens, blue – R substituents. See text for the explanation of cluster symbols.

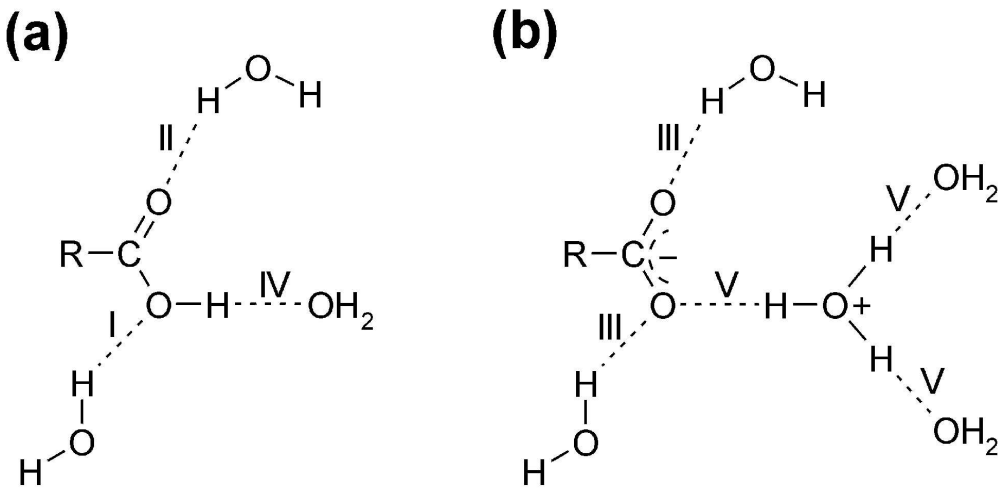

Figure 5. Schematic R-COOH aqueous clusters in (a) neutral and (b) contact ion pair arrangement, with hydrogen bonds indicated by dashed lines. The Roman numbers over hydrogen bonds refer to hydrogen bond types listed in Table 2.